

## THE MASS SURFACE DENSITY IN THE LOCAL DISK AND THE CHEMICAL EVOLUTION OF THE GALAXY

DONATELLA ROMANO, FRANCESCA MATTEUCCI<sup>1</sup>, PAOLO SALUCCI  
 SISSA/ISAS, via Beirut 2-4, I-34014 Trieste, Italy; romano, salucci@sissa.it

AND

CRISTINA CHIAPPINI

Departamento de Astronomia, Observatório Nacional/CNPq, Caixa Postal 23002, Rio de Janeiro, RJ, Brazil;  
 chiappini@danw.on.br

*Received 2000 January 19; accepted 2000 March 8*

### ABSTRACT

We have studied the effect of adopting different values of the total baryonic mass surface density in the local disk at the present time,  $\Sigma(R_\odot, t_{Gal})$ , in a model for the chemical evolution of the Galaxy. We have compared our model results with the G-dwarf metallicity distribution, the amounts of gas, stars, stellar remnants, infall rate and SN rate in the solar vicinity, and with the radial abundance gradients and gas distribution in the disk. This comparison strongly suggests that the value of  $\Sigma(R_\odot, t_{Gal})$  which best fits the observational properties should lie in the range  $50 - 75 M_\odot \text{ pc}^{-2}$ , and that values of the total disk mass surface density outside this range should be ruled out.

*Subject headings:* Galaxy: evolution — Galaxy: stellar content — Galaxy: structure — dark matter

### 1. INTRODUCTION

Despite a number of estimates, obtained by means of several different methods, the value of the local column density of the Galactic disk in stars and gas,  $\Sigma_b(R_\odot \simeq 8 \text{ kpc}) = \Sigma_{stars} + \Sigma_{gas}$ , has been until recently very uncertain. Direct HST star counts imply a stellar column density of  $\simeq 27 M_\odot \text{ pc}^{-2}$  (Flynn, Gould, & Bahcall 1999), while the (H I + H<sub>2</sub>) column density amounts to  $7 - 13 M_\odot \text{ pc}^{-2}$  (Dickey 1993; Flynn et al. 1999). Therefore, the surface density of the directly seen baryonic matter amounts to  $35 - 40 M_\odot \text{ pc}^{-2}$ . However, the actual column density of the “luminous” disk could be higher because the above detection does not account for dead stars and brown dwarfs.

The total disk surface density  $\Sigma_z(R_\odot)$ , including also any eventual disk dark matter component, can be determined from the motion of stars in the solar neighborhood perpendicular to the Galactic plane (e.g. Binney & Tremaine 1987; Gilmore, Wyse, & Kuijken 1989). From the kinematics of a sample of K-giants Bahcall, Flynn, & Gould (1992) derived  $\Sigma_z(R_\odot) = 84^{+30}_{-25} M_\odot \text{ pc}^{-2}$  (at  $1\sigma$  level). Notice that such a measure is a complex one and it is strongly dependent on the underlying assumptions. By employing different samples and/or analysis, lower values for  $\Sigma_z(R_\odot)$  have been claimed:  $\Sigma_z(R_\odot) = 46 \pm 9 M_\odot \text{ pc}^{-2}$  (Kuijken & Gilmore 1989) — revised to  $48 \pm 9 M_\odot \text{ pc}^{-2}$  (Kuijken & Gilmore 1991),  $\Sigma_z(R_\odot) = 52 \pm 13 M_\odot \text{ pc}^{-2}$  (Flynn & Fuchs 1994). The local column density of stars and gas could be smaller, because these dynamical estimates may include some non-baryonic matter. Notice however that it is quite unlikely that there is non-baryonic matter in the disk, because non-baryonic dark matter is probably non dissipational. Any non-baryonic matter present in the disk is likely to be part of the dark halo, and this component is always subtracted from the

dynamical estimates of the local column density.

Fitting the Galaxy rotation curve (RC) with a mass model provides a further way of estimating the local column density of disk matter  $\Sigma_V$ . In fact, such a fit indicates what is the fraction  $\beta^2$  of the circular velocity due to the disk component (at the Sun’s position). Then,  $\beta V_\odot^2$  is compared with the circular velocity of an exponential thin disk,  $V_{disk}^2 = G^{-1} \Sigma_V R_D f(R_\odot/R_D)$ , with  $f$  a known function of the Galactocentric distance of the Sun expressed in terms of disk length scales (see Freeman 1970), to yield  $\Sigma_V$ , providing that  $R_\odot$  and  $R_D$  are known. The results are far from unique, and reflect the presence of uncertainties in the mass modelling, in the actual shape of the Galactic RC, and in the basic structural parameters. The values found range between  $\Sigma_V \sim 50 M_\odot \text{ pc}^{-2}$  and  $\sim 100 M_\odot \text{ pc}^{-2}$  (Olling & Merrifield 1998; Dehnen & Binney 1998), and moreover include any dark matter distributed like the stellar disk. In external galaxies of luminosity similar to the Galaxy ( $L_B \sim 10^{11} L_\odot$ ), values of  $\Sigma_V$  as high as  $\simeq 90 M_\odot \text{ pc}^{-2}$  at  $R = 8 \text{ kpc}$  cannot be ruled out (Persic, Salucci, & Stel 1996).

Finally, let us note that if the dark matter halo in the Galaxy follows the standard cold dark matter (CDM) universal density profile (Navarro, Frenk, & White 1997), and therefore at the Sun position  $\rho_{SCDM} \propto R^{-2}$ , then the local disk column density is required to be towards the low end of the above-cited values (e.g. Courteau & Rix 1999). On the other hand, low- $\Omega$  CDM density profiles are not inconsistent with a baryon dominated region inside  $R_\odot$ , and then with much higher values for the local disk column density (Navarro 1998).

Summarizing: all the above observations, often entangled with heavy theoretical assumptions, poorly constrain the value of the column density of the baryonic matter in

<sup>1</sup>Dipartimento di Astronomia, Università di Trieste, via G.B. Tiepolo 11, I-34131 Trieste, Italy; matteucci@ts.astro.it

<sup>2</sup>It should be noted that the value for  $\beta$  depends on the assumed profiles for the disk and the halo.

the local disk, that may lie between 35 and  $100 M_{\odot} \text{ pc}^{-2}$ .

However, very recently the results of the European Space Agency's Hipparcos mission have allowed a drastic reduction of this permitted range, by making available direct distances for the tracer stars. In particular, Crézé et al. (1998) and Holmberg & Flynn (1998) have analyzed the A and F stars in the Hipparcos data set (some 10,000 stars) and derived greatly improved estimates of the total gravitating mass: the gravitating disk mass seems to be now firmly established at 50 to  $60 M_{\odot} \text{ pc}^{-2}$ .

In this paper we investigate how the gravitating mass of the disk influences the Galactic chemical evolution. Successful models for the chemical evolution of the Galaxy, in fact, require a star formation law depending on the total mass surface density (Tosi 1988; Matteucci & François 1989; Chiappini, Matteucci, & Gratton 1997), and the star formation rate (SFR) is a fundamental parameter in the evolution of galaxies.

## 2. THE CHEMICAL EVOLUTION MODEL

We adopt the two-infall chemical evolution model of Chiappini et al. (1997), to which we refer for an exhaustive explanation of the main assumptions and basic equations. Here we just review the features of the model most directly related to the aspects discussed in the present study.

Briefly, the overall evolutionary scenario is the following: it is assumed that the Galaxy formed out of two main infall episodes; during the first episode, the primordial gas collapsed very quickly and formed the spheroidal components (halo and bulge); during the second episode, the thin disk formed almost independently of the previous infall episode, mainly out of material of primordial chemical composition. The disk formation process is assumed to be slower with increasing Galactocentric distance (Larson 1976; Matteucci & François 1989); this "inside-out" formation of the Galactic disk is required to reproduce the abundance gradients and the gas distribution along the disk. A hiatus in the star formation between thick disk and thin disk phases, as suggested by recent observations (Gratton et al. 1996; Bernkopf & Fuhrmann 1998; Fuhrmann 1998; Carraro 2000), is naturally produced by the model under the assumption that the star formation stops when the gas surface density drops below a threshold of  $7 M_{\odot} \text{ pc}^{-2}$  (Kennicutt 1989). Moreover, the presence of such a threshold predicts a roughly constant gas density profile at the outer radii (between 8 and 14 kpc) in agreement with observations (Dame 1993). We will focus on the thin disk formation process.

The most relevant quantities in the present discussion are the infall rate and the SFR, since they involve the total mass surface density profile. The rate at which the thin disk is formed out of external matter (although it has also some initial contribution from the halo gas) is:

$$\frac{d\Sigma_I(R, t)}{dt} = B(R) e^{-(t-t_{max})/\tau_D}, \quad (1)$$

where  $\Sigma_I(R, t)$  is the gas surface density of the infalling material, which has a primordial chemical composition;  $t_{max}$  is the time of maximum gas accretion onto the disk, coincident with the end of the halo-thick disk phase which is set equal to 1 Gyr;  $\tau_D$  is the timescale for mass accretion onto the thin disk component. We assume that  $\tau_D$

increases with increasing the Galactic radius:

$$\tau_D(R) = 1.033 \times R - 1.267. \quad (2)$$

This relation derives from the fact that in order to fit the G-dwarf metallicity distribution in the solar neighborhood it is necessary to assume  $\tau_D = 7$  Gyr, whereas to reproduce the metallicity distribution of the stars in the Galactic bulge ( $R = 2$  kpc) a timescale  $\tau_D = 0.8$  Gyr is required (Matteucci, Romano, & Molaro 1999). It should be emphasized that this choice also guarantees a good fit to the gas density profile and to the Galactic abundance gradients. The quantity  $B(R)$  is derived from the condition of reproducing the current total mass surface density distribution along the disk:

$$B(R) = \frac{\Sigma(R, t_{Gal})}{\tau_D(R) \left(1 - e^{-(t_{Gal}-t_{max})/\tau_D(R)}\right)}. \quad (3)$$

$t_{Gal} = 15$  Gyr is the age of the Galaxy starting with the formation of the halo. From equation (3) it is clear the strong dependence of the infall rate from the total mass density profile.

Observations in our own and in other disk galaxies allow us to relate the SFR to intrinsic parameters of galaxies, in particular to the average surface gas density:  $\text{SFR} \propto \Sigma_{gas}^k$  (Schmidt 1959), where the exponent is reasonably well known (e.g.  $k = 1.4 \pm 0.15$  — Kennicutt 1998). Moreover, the correlation between metallicity and surface brightness noted for late type spirals (McCall 1982; Edmunds & Pagel 1984; Dopita & Ryder 1994) is consistent with theories of self-regulated star formation, in which the energy produced by young stars and SNe feeds back into the ISM and inhibits further star formation by producing an expansion of the region surrounding the new stars or the SN remnants, thus relating the SFR to the gravitational potential and therefore to the total mass surface density. In addition, according to the most popular prescriptions, one of the key conditions for star formation to occur is

$$t_{cooling} \ll t_{ff}, \quad (4)$$

where  $t_{cooling}$  is the cooling timescale and  $t_{ff}$  is the free-fall timescale (Katz 1992; Navarro & White 1993; Carraro, Lia, & Chiosi 1998);  $t_{ff} \propto \rho^{-1/2}$ , where  $\rho$  is the total mass density (Buonomo et al. 1999). Again, in some way the SFR is related to the potential well and therefore to the total mass surface density. The SFR adopted here is the same as in Chiappini et al. (1997) and it was chosen in order to give the best agreement with the observed constraints:

$$\psi(R, t) = \nu(t) \left( \frac{\Sigma(R, t)}{\Sigma(R_{\odot}, t)} \right)^{2(k-1)} \left( \frac{\Sigma(R, t_{Gal})}{\Sigma(R, t)} \right)^{k-1} \cdot \Sigma_{gas}^k(R, t). \quad (5)$$

$\nu(t)$  is the efficiency of the star formation process, which is set to  $1 \text{ Gyr}^{-1}$ , except when the gas surface density drops below  $7 M_{\odot} \text{ pc}^{-2}$ . In fact in this case  $\nu(t) = 0$ , because below this critical density the gas is gravitationally stable against density condensations into stars.  $\Sigma(R, t)$  is the total disk mass surface density at a given radius  $R$  and a

TABLE 1

Comparison between model predictions and observations for some relevant current quantities.

Quantity	35	54	80	100	Observations	Reference
Type I SNe (century <sup>-1</sup> )	0.27	0.37	0.59	0.72	0.17–0.7	1
Type II SNe (century <sup>-1</sup> )	0.73	0.95	1.67	2.06	0.55–2.2	1
Nova outbursts (yr <sup>-1</sup> )	20	27	35	41	20–30	2
SFR ( $R_{\odot}, t_{Gal}$ ) ( $M_{\odot}$ pc <sup>-2</sup> Gyr <sup>-1</sup> )	0–3	2.57	2.89	3.58	2–10	3
$\Sigma_{gas}$ ( $R_{\odot}, t_{Gal}$ ) ( $M_{\odot}$ pc <sup>-2</sup> )	7.0	7.0	8.4	10.3	7–13	4
$\Sigma_{stars}$ ( $R_{\odot}, t_{Gal}$ ) ( $M_{\odot}$ pc <sup>-2</sup> )	25.5	38.4	54.3	65.6	35 ± 5	5
$\Sigma_{remnants}$ ( $R_{\odot}, t_{Gal}$ ) ( $M_{\odot}$ pc <sup>-2</sup> )	2.5	8.6	17.3	24.0	2–4	6
$\dot{\Sigma}_{infall}$ ( $R_{\odot}, t_{Gal}$ ) ( $M_{\odot}$ pc <sup>-2</sup> Gyr <sup>-1</sup> )	0.57	0.89	1.32	1.66	0.3–1.5	7

REFERENCES.—(1) Chiappini et al. 1997 and references therein; (2) Shafter 1997; (3) Güsten & Mezger 1982; (4) Dickey 1993; Flynn et al. 1999; (5) Gilmore et al. 1989; (6) Méra, Chabrier, & Schaeffer 1998 quote  $\Sigma_{WDS+NSs} = 2–4 M_{\odot}$  pc<sup>-2</sup>; here  $\Sigma_{remnants} = \Sigma_{WDS+NSs+BHs}$ ; (7) Portinari, Chiosi, & Bressan 1998 and references therein

given time  $t$ ,  $\Sigma(R_{\odot}, t)$  is the total disk mass surface density at the Solar position and  $\Sigma_{gas}(R, t)$  is the gas surface density. Note that the gas surface density exponent,  $k$ , equal to 1.5, was obtained from the best model of Chiappini et al. (1997) in order to ensure a good fit to the observational constraints at the solar vicinity. This value is in good agreement with the recent observational results of Kennicutt (1998) and with N-body simulation results by Gerritsen & Icke (1997).

As far as our present model is concerned, we stress that the SFR *along the Galactic disk*, and hence the evolutionary history of the Galactic disk itself, is fixed by the *specific value of the local column density* of disk matter that we adopt. In fact, the total disk mass surface density profile, an exponential with scale length  $R_D$ , can be expressed as:

$$\Sigma(R, t_{Gal}) = \Sigma(R_{\odot}, t_{Gal}) \cdot e^{-(R-R_{\odot})/R_D}, \quad (6)$$

which relates the column density at a radius  $R$  to the column density at the Solar position. For the purpose of this paper, we let the local mass surface density value to vary from 35 to 100  $M_{\odot}$  pc<sup>-2</sup> and we set  $R_{\odot} = 8$  kpc.

Finally, the stellar nucleosynthesis prescriptions we adopt are from:

- van den Hoek & Groenewegen (1997) for low-intermediate mass stars ( $0.8–8 M_{\odot}$ ) (their case with variable  $\eta_{AGB}$ );
- Charbonnel & do Nascimento (1998) for  $^3\text{He}$  production/destruction in low-mass stars ( $M < 2 M_{\odot}$ );
- Woosley & Weaver (1995) for Type II SNe ( $M > 10 M_{\odot}$ );
- Thielemann, Nomoto, & Hashimoto (1993) for Type Ia SNe (exploding white dwarfs in binary systems as described in Matteucci & Greggio 1986);
- José & Hernanz (1998) for classical novae.

Our prescriptions differ from those of Chiappini et al. (1997) in: i) the range of low-intermediate masses ( $0.8–8 M_{\odot}$ ), where they adopted the Renzini & Voli (1981)

yields; ii) the fact that we are including the explosive nucleosynthesis from nova outbursts (Romano et al. 1999; Romano & Matteucci 2000); iii) using extra-mixing prescriptions for the  $^3\text{He}$  nucleosynthesis (Chiappini & Matteucci 2000) and iv) the Sun position, now taken as 8 kpc instead of 10 kpc.

As far as the composition of the infalling material is concerned, we set  $Y_P = 0.245$  rather than 0.23 (where  $Y_P$  is the primordial mass fraction in form of  $^4\text{He}$ ), according to a recent estimate of the pristine  $^4\text{He}$  abundance obtained as a weighted mean of the  $^4\text{He}$  mass fractions from the two most metal-deficient blue compact galaxies, corrected for the stellar contribution ( $Y_P = 0.245 \pm 0.002$  — Izotov et al. 1999<sup>3</sup>). The primordial abundances by mass of deuterium and helium-3 are  $D_P = 4.5 \times 10^{-5}$  and  $^3\text{He}_P = 4.0 \times 10^{-5}$ , respectively. The adopted IMF is that of Scalo (1986).

### 3. MODEL PREDICTIONS

#### 3.1. The Solar Circle

In Tables 1 and 2 the model predictions together with the corresponding observed quantities are shown. Different models have identical parameters apart from the value of  $\Sigma(R_{\odot})$ .

From an inspection of Table 1, we see that there are not big differences among the quantities predicted by the different models, with the exception of the surface densities of live stars and stellar remnants, which seem to exclude the models with the highest total disk mass surface densities ( $80–100 M_{\odot}$  pc<sup>-2</sup>). The lowest density value ( $35 M_{\odot}$  pc<sup>-2</sup>) predicts a stellar density which is only in marginal agreement with the observed one.

The predictions on the abundances of the interstellar medium at the time of the Sun's formation are independent of the chosen total disk mass surface density but depend on all other model assumptions, in particular on the assumed stellar yields. Therefore, since we adopted a set of new yields relative to Chiappini et al. (1997), a comparison between our results for  $\Sigma = 54 M_{\odot}$  pc<sup>-2</sup> and those

<sup>3</sup>Ionization corrections for low-metallicity H II regions suggest that this estimate should be reduced to  $Y_P = 0.241 \pm 0.002$  (Viegas, Gruenwald, & Steigman 1999).

TABLE 2

Theoretical solar abundances (mass fraction) are compared to the observed ones (Anders & Grevesse 1989).

$X_i$	This paper	Chiappini et al. 1997	Observed
H	0.710	0.731	0.706
D	$3.231 \times 10^{-5}$	$4.630 \times 10^{-5}$	$4.80 \times 10^{-5}$
$^3\text{He}$	$3.277 \times 10^{-5}$	$10.01 \times 10^{-5}$	$2.93 \times 10^{-5}$
$^4\text{He}$	0.273	0.255	0.275
$^7\text{Li}$	$8.740 \times 10^{-9}$	...	$9.63 \times 10^{-9}$
$^{12}\text{C}$	$3.920 \times 10^{-3}$	$1.827 \times 10^{-3}$	$3.03 \times 10^{-3}$
$^{13}\text{C}$	$5.215 \times 10^{-5}$	$4.758 \times 10^{-5}$	$3.65 \times 10^{-5}$
$^{14}\text{N}$	$1.670 \times 10^{-3}$	$1.386 \times 10^{-3}$	$1.11 \times 10^{-3}$
$^{16}\text{O}$	$7.378 \times 10^{-3}$	$7.278 \times 10^{-3}$	$9.59 \times 10^{-3}$
$^{20}\text{Ne}$	$9.729 \times 10^{-4}$	$9.42 \times 10^{-4}$	$1.62 \times 10^{-3}$
$^{24}\text{Mg}$	$2.563 \times 10^{-4}$	$2.48 \times 10^{-4}$	$5.15 \times 10^{-4}$
Si	$7.348 \times 10^{-4}$	$7.03 \times 10^{-4}$	$7.11 \times 10^{-4}$
S	$3.220 \times 10^{-4}$	$3.071 \times 10^{-4}$	$4.18 \times 10^{-4}$
Ca	$4.145 \times 10^{-5}$	$3.95 \times 10^{-5}$	$6.20 \times 10^{-5}$
Fe	$1.467 \times 10^{-3}$	$1.37 \times 10^{-3}$	$1.27 \times 10^{-3}$
Cu	$8.920 \times 10^{-7}$	$8.18 \times 10^{-7}$	$8.40 \times 10^{-7}$
Zn	$2.635 \times 10^{-6}$	$2.44 \times 10^{-6}$	$2.09 \times 10^{-6}$
Z	$1.700 \times 10^{-2}$	$1.433 \times 10^{-2}$	$1.886 \times 10^{-2}$

of Chiappini et al. (1997) is required. Table 2 shows that the largest differences in the predicted solar abundances arise for D,  $^3\text{He}$ ,  $^{12}\text{C}$ , and  $^{13}\text{C}$ . The improvement in the predicted solar abundance for  $^{12}\text{C}$  and  $^{13}\text{C}$  is due to the fact that we adopt the new nucleosynthetic yields from van den Hoek & Groenewegen (1997) for low and intermediate mass stars, whereas the improvement in the predicted solar abundances for D and  $^3\text{He}$  is due to the fact that we take into account that 93% of evolved stars undergo the extra-mixing on the RGB and thus destroy, at least partly, their  $^3\text{He}$  (Charbonnel & do Nascimento 1998).

One of the most severe observational constraints to chemical evolution models is the relative number of stars formed at a given time, i.e. at a given metallicity. In Fig.1 we compare the predicted and observed G-dwarf metallicity distributions; in particular, we show the results of models in which  $\Sigma(R_\odot, t_{Gal})$  is taken to be 20, 54 and 100  $M_\odot \text{ pc}^{-2}$ , respectively. Models with  $\Sigma = 35$  and  $80 M_\odot \text{ pc}^{-2}$  have also been computed. They produce theoretical G-dwarf distributions very similar to those obtained with  $\Sigma = 54$  or  $100 M_\odot \text{ pc}^{-2}$ , so we do not show them here. From an inspection of Fig.1 we see that the case  $\Sigma = 20 M_\odot \text{ pc}^{-2}$  is in trouble in reproducing the high metallicity tail of the distribution while overestimating the number of low metallicity stars, whereas all the cases with  $\Sigma$  lying between 35 and 100  $M_\odot \text{ pc}^{-2}$  lead to a better agreement with the observations. We performed a  $\chi^2$  test and obtained the following results:  $\chi^2 = 0.11$  for the case  $\Sigma = 20 M_\odot \text{ pc}^{-2}$ ,  $\chi^2 = 0.04$  for the cases  $\Sigma = 54$  and  $100 M_\odot \text{ pc}^{-2}$ . We conclude that the observed differential metallicity distribution is not a useful tool to distinguish among realistic values for the total baryonic mass density in the local disk. This is not surprising since the G-dwarf metallicity distribution depends mostly on the assumed law for the disk formation (i.e. on the assumed infall timescale).

Fig.2 illustrates the different temporal behaviour of the SFR under different choices of  $\Sigma$ . In the low density case a stochastic SFR (between 0 and  $3 M_\odot \text{ pc}^{-2}$

$\text{Gyr}^{-1}$  at the present time) is expected during most of the evolution, due to the fact that the threshold in the gas density, below which the star formation stops, is easily attained in this case. On the other hand, in the case of a very high  $\Sigma$  the star formation process is not able to consume enough gas to go below the threshold. This explains why the highest  $\Sigma$  values produce the high stellar and remnant densities listed in Table 1. In a recent paper Rocha-Pinto et al. (2000) suggest that

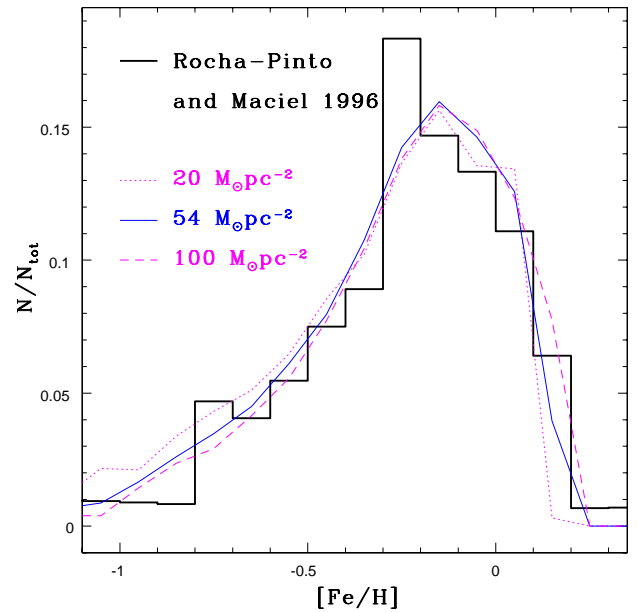


FIG. 1.— Theoretical G-dwarf distributions obtained by choosing different values of  $\Sigma(R_\odot, t_{Gal})$  as input parameters in the chemical evolution model compared to the observed one (Rocha-Pinto & Maciel 1996). The [Fe/H] ratios are normalised to the theoretical solar one for each model.

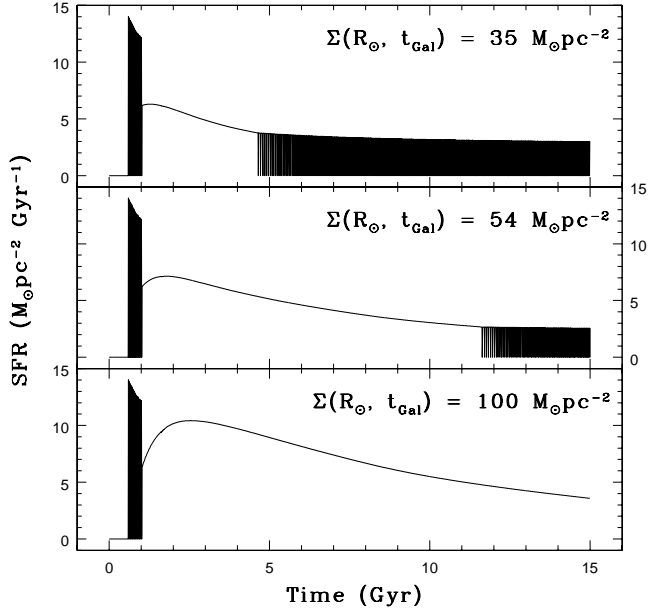


FIG. 2.— Temporal evolution of the star formation rate in the solar vicinity as predicted by models adopting  $\Sigma(R_\odot, t_{Gal}) = 35, 54$ , and  $100 M_\odot \text{ pc}^{-2}$ .

the SFR in the disk should have proceeded in three distinct bursts at 0–1, 2–5, and 7–9 Gyr ago. The earliest episode of enhanced star formation should reflect the beginning of the solar vicinity formation (and probably corresponds to our maximum infall time). The other two episodes could be related to cyclical mechanisms (for instance, tidal interactions between the Galaxy and the Magellanic Clouds, or even induced star formation by spiral arms). As already explained, the theoretical G-dwarf metallicity distribution is mainly dependent on the assumed timescale for the formation of the solar vicinity, hence it would not be too much affected by recent bursts of star formation.

The elemental abundance ratios as a function of metallicity are nearly independent of the adopted  $\Sigma$  value, depending mostly on the nucleosynthetic yields and the initial mass function. Therefore we do not discuss them here.

### 3.2. Radial Profiles

Here we discuss the predicted radial properties, in order to investigate the model behaviour along the overall Galactic disk under different prescriptions on the value of  $\Sigma(R_\odot)$ .

We assume that the radial surface density distribution of the disk is exponential (see Sect.2, equation (6)), and run models assuming different values for the exponential scale length,  $R_D$ . Fig.3 shows the radial distribution of the present day surface gas density as predicted by models adopting  $R_D = 2.5, 3.5$ , and  $4.5 \text{ kpc}$  (dashed, solid, and dotted lines, respectively), for different  $\Sigma$  values. The model predictions are compared with the observed gas distribution derived by Dame (1993).

<sup>4</sup>A scale length value of 3.5 kpc is the preferred one, being able to produce a final stellar density scale length in agreement with the observed one (2.5–3.0 kpc — Sackett 1997; Freudenreich 1998).

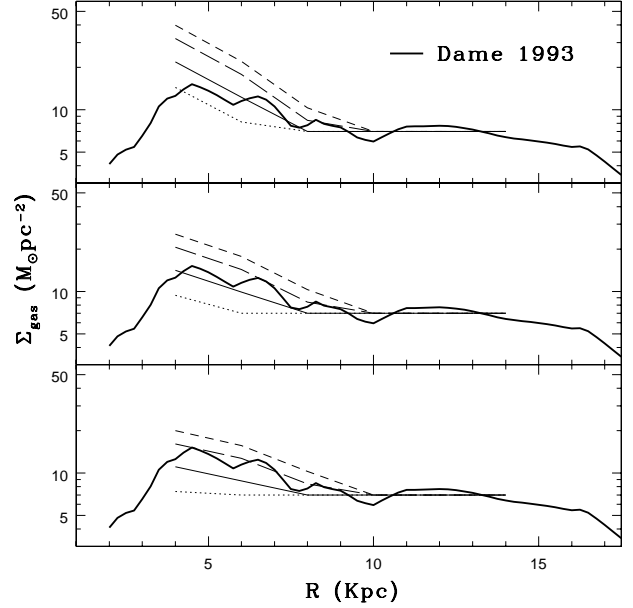


FIG. 3.— Radial distribution of the present day surface gas density as predicted by models with  $R_D = 2.5$  (upper panel),  $R_D = 3.5$  (middle panel), and  $R_D = 4.5$  (lower panel). From bottom to top, for each of these panels: lines referring to  $\Sigma(R_\odot, t_{Gal}) = 35, 54, 80$ , and  $100 M_\odot \text{ pc}^{-2}$  (dotted, continuous, long-dashed, and short-dashed lines, respectively). The observed ( $\text{H I} + \text{H}_2$ ) distribution is taken from Dame (1993). The surface density distribution of the total gas  $\Sigma_{gas}$  is obtained from the sum of the  $\text{H I}$  and  $\text{H}_2$  distributions,  $\Sigma_{HI} + \Sigma_{H_2}$ , accounting for the helium and heavy elements fractions (thick line).

All our models predict a flattening of the distribution at radii larger than 10 kpc, due to the presence of the threshold star formation density. Models with  $\Sigma = 35 M_\odot \text{ pc}^{-2}$  give a flat gas distribution already at the smallest radii; on the contrary, models with  $\Sigma = 100 M_\odot \text{ pc}^{-2}$  produce very steep distributions, hardly compatible with observations. All models predict that the gas content increases toward the Galactic center, whereas the observations clearly show a decreasing trend below 5 kpc. This problem could be solved by including the Galactic bar (e.g. Portinari & Chiosi 2000), not present in the model. Taking into account these uncertainties we can conclude that the best gas distribution is obtained for local values of the total mass surface density in the range  $50 - 75 M_\odot \text{ pc}^{-2}$ .

We also notice how increasing the disk scale length from 2.5 to 4.5 leads to a flattening in the predicted distribution. This behaviour is also observed in the case of the predicted radial density distributions of stars<sup>4</sup>, stellar remnants, and in the case of the predicted abundance gradients. In particular, higher total mass densities and larger scale lengths tend to flatten the gradients in the external regions of the disk. The actual situation is still controversial, with observations partly supporting this flattening (Vilchez & Esteban 1996; Maciel & Quireza 1999) and partly not (Afferbach, Churchwell, & Werner 1997; Smartt & Rolleston 1997; Rudolph et al. 1997). Therefore we can not draw any firm conclusion on this point.

#### 4. CONCLUSIONS

We used a detailed model of galactic chemical evolution applied to our own galaxy in order to put constraints on the total amount of disk baryonic matter. Observational estimates of this quantity in the local disk span a wide range of values (from 35 to  $100 M_{\odot} \text{ pc}^{-2}$ ), depending on the underlying theoretical assumptions and on the adopted methods. We show that by means of chemical evolution models it is possible to substantially restrict the observed range of the total mass surface density.

We show that the value of  $\Sigma(R_{\odot})$  should be restricted to the range  $50 - 75 M_{\odot} \text{ pc}^{-2}$ , in order to guarantee the best fit to all the observational constraints available for the solar neighborhood and the overall Galactic disk. This is well consistent with the mass range which Crézé et al. (1998)

and Holmberg & Flynn (1998) advocate from their analysis of A and F stars with parallaxes and proper motions from the Hipparcos satellite.

We would like to thank Dennis W. Sciama for enlightening comments and Cedric G. Lacey for careful reading of the manuscript. We would like also to thank the referee, Dr. Chris Flynn, for many comments that improved the presentation of the paper. D.R. wish to thank Cesario Lia for discussing the feed-back mechanism. F.M. and P.S. acknowledge financial support from the Italian Ministry for University and for Scientific and Technological Research (MURST). C.C. wish to thank Thomas M. Dame for having kindly sent his data on the gas density distribution along the disk and to acknowledge financial support from CNPq/Brazil.

#### REFERENCES

Afflerbach, A., Churchwell, E., & Werner, M.W. 1997, *ApJ*, 478, 190  
 Anders, E., & Grevesse, N. 1989, *Geochim. Cosmochim. Acta*, 53, 197  
 Bahcall, J.N., Flynn, C., & Gould, A. 1992, *ApJ*, 389, 234  
 Bernkopf, J., & Fuhrmann, K. 1998, in *Galaxy Evolution: Connecting the Distant Universe with the Local Fossil Record*, ed. M. Spite, & F. Cribo (Kluwer: Dordrecht), 43  
 Binney, J., & Tremaine, S. 1987, *Galactic dynamics* (Princeton: Princeton Univ. Press)  
 Buonomo, F., Carraro, G., Chiosi, C., & Lia, C. 1999, *MNRAS*, in press (astro-ph/9909199)  
 Carraro, G. 2000, in *The Chemical Evolution of the Milky Way: Stars versus Clusters*, ed. F. Giovannelli, & F. Matteucci (Kluwer: Dordrecht), in press (astro-ph/9911382)  
 Carraro, G., Lia, C., & Chiosi, C. 1998, *MNRAS*, 297, 1021  
 Charbonnel, C., & do Nascimento, J.D., Jr. 1998, *A&A*, 336, 915  
 Chiappini, C., & Matteucci, F. 2000, in *ASP Conf. Ser.*, The Light Elements and their Evolution, ed. L. da Silva, R. de Medeiros, & M. Spite (San Francisco: ASP), in press  
 Chiappini, C., Matteucci, F., & Gratton, R. 1997, *ApJ*, 477, 765  
 Courteau, S., & Rix, H.-W. 1999, *ApJ*, 513, 561  
 Crézé, M., Chereul, E., Bienaymé, O., & Pichon, C. 1998, *A&A*, 329, 920  
 Dame, T.M. 1993, in *Back to the Galaxy*, ed. S. Holt, & F. Verter, 267  
 Dehnen, W., & Binney, J.J. 1998, *MNRAS*, 298, 387  
 Dickey, J.M. 1993, in *ASP Conf. Ser.* 39, The Minnesota Lectures on the Structure and Dynamics of the Milky Way, ed. R.M. Humphreys (San Francisco: ASP), 93  
 Dopita, M.A., & Ryder, S.D. 1994, *ApJ*, 430, 163  
 Edmunds, M.G., & Pagel, B.E.J. 1984, *MNRAS*, 211, 507  
 Flynn, C., & Fuchs, B. 1994, *MNRAS*, 270, 471  
 Flynn, C., Gould, A., & Bahcall, J.N. 1999, in *ASP Conf. Ser.* 165, The Third Stromlo Symposium: The Galactic Halo, ed. B.K. Gibson, T.S. Axelrod, & M.E. Putman (San Francisco: ASP), 387  
 Freeman, K.C. 1970, *ApJ*, 160, 811  
 Freudenreich, H.T. 1998, *ApJ*, 492, 495  
 Fuhrmann, K. 1998, *A&A*, 338, 161  
 Gerritsen, J.P.E., & Icke, V. 1997, *A&A*, 325, 972  
 Gilmore, G., Wyse, R.F.G., & Kuijken, K. 1989, *ARA&A*, 27, 555  
 Gratton, R., Carretta, E., Matteucci, F., & Sneden, C. 1996, in *ASP Conf. Ser.* 92, Formation of the Galactic Halo — Inside and Out, ed. H. Morrison, A. Sarajedini (San Francisco: ASP), 307  
 Güsten, R., & Mezger, P.G. 1982, *Vistas Astron.*, 26, 159  
 Holmberg, J., & Flynn, C. 1998, *MNRAS*, submitted (astro-ph/9812404)  
 Izotov, Y.I., Chaffee, F.H., Foltz, C.B., Green, R.F., Guseva, N.G., & Thuan, T.X. 1999, *ApJ*, 527, 7571  
 José, J., & Hernanz, M. 1998, *ApJ*, 494, 680  
 Katz, N. 1992, *ApJ*, 391, 502  
 Kennicutt, R.C., Jr. 1989, *ApJ*, 344, 685  
 Kennicutt, R.C., Jr. 1998, *ApJ*, 498, 541  
 Kuijken, K., & Gilmore, G. 1989, *MNRAS*, 239, 605  
 Kuijken, K., & Gilmore, G. 1991, *ApJ*, 367, L9  
 Larson, R.B. 1976, *MNRAS*, 176, 31  
 Maciel, W.J., & Quireza, C. 1999, *A&A*, 345, 629  
 Matteucci, F., & François, P. 1989, *MNRAS*, 239, 885  
 Matteucci, F., & Gregg, L. 1986, *A&A*, 154, 279  
 Matteucci, F., Romano, D., & Molaro, P. 1999, *A&A*, 341, 458  
 McCall, M.L. 1982, PhD Thesis, The Univ. of Texas at Austin  
 Méra, D., Chabrier, G., & Schaeffer, R. 1998, *A&A*, 330, 937  
 Navarro, J.F. 1998, *ApJ*, submitted (astro-ph/9807084)  
 Navarro, J.F., Frenk, C.S., & White, S.D.M. 1997, *ApJ*, 490, 493  
 Navarro, J.F., & White, S.D.M. 1993, *MNRAS*, 265, 271  
 Olling, R.P., & Merrifield, M.R. 1998, *MNRAS*, 299, 430  
 Persic, M., Salucci, P., & Stel, F. 1996, *MNRAS*, 281, 27  
 Portinari, L., & Chiosi, C. 2000, *A&A*, in press (astro-ph/0002145)  
 Portinari, L., Chiosi, C., & Bressan, A. 1998, *A&A*, 334, 505  
 Renzini, A., & Voli, M. 1981, *A&A*, 94, 175  
 Rocha-Pinto, H.J., & Maciel, W.J. 1996, *MNRAS*, 279, 447  
 Rocha-Pinto, H.J., Scalo, J., Maciel, W.J., & Flynn, C. 2000, *A&A*, submitted (astro-ph/0001383)  
 Romano, D., & Matteucci, F. 2000, in *The Chemical Evolution of the Milky Way: Stars versus Clusters*, ed. F. Giovannelli, & F. Matteucci (Kluwer: Dordrecht), in press (astro-ph/0001253)  
 Romano, D., Matteucci, F., Molaro, P., & Bonifacio, P. 1999, *A&A*, 352, 117  
 Rudolph, A.L., Simpson, J.P., Haas, M.R., Erickson, E.F., & Fich, M. 1997, *ApJ*, 489, 94  
 Sackett, P.D. 1997, *ApJ*, 483, 103  
 Scalo, J.M. 1986, *Fund. Cosmic Phys.*, 11, 1  
 Schmidt, M. 1959, *ApJ*, 129, 243  
 Shafter, A.W. 1997, *ApJ*, 487, 226  
 Smartt, S.J., & Rolleston, W.R.J. 1997, *ApJ*, 481, L47  
 Thielemann, F.K., Nomoto, K., & Hashimoto, M. 1993, in *Origin and Evolution of the Elements*, ed. N. Prantzos, E. Vangioni-Flam, & M. Cassé (Cambridge: Cambridge Univ. Press), 297  
 Tosi, M. 1988, *A&A*, 197, 33  
 van den Hoek, L.B., & Groenewegen, M.A.T. 1997, *A&AS*, 123, 305  
 Viegas, S.M., Gruenwald, R., & Steigman, G. 1999, *ApJ*, in press (astro-ph/9909213)  
 Vilchez, J.M., & Esteban, C. 1996, *MNRAS*, 280, 720  
 Woosley, S.E., & Weaver, T.A. 1995, *ApJS*, 101, 181